Chapter 3

INTELLIGENT SCHEDULING OF PEVS FOR CUSTOMER BENEFITS, AND PROVIDING VOLTAGE SUPPORT TO THE MICRO-GRID

3.1 INTRODUCTION

Electric Vehicle (EV) is considered an alternative to the traditional internal combustion-based vehicle as it has higher energy conversion efficiency and reduced carbon footprints. The Council on Energy, Environment, and Water (CEEW) report suggests that if electric vehicles attain 30% of India's vehicle sales by 2030, a 17% reduction in particulate matter, 18% in CO emissions, and 4% in greenhouse gases can be achieved [94]. The recent developments in battery technology and universally available power systems have led to the widespread availability of EVs at several price segments. Moreover, the economic incentives for the EV owners where the charger is capable of bi-directional power flow have motivated customers to adopt electric mobility.

However, the impact of a large number of EVs on the grid is an interesting aspect to be discovered. While charging, EVs consume a considerable amount of energy and share a substantial segment in the load profile. Although the influence of a single Plug-in Electric Vehicle (PEV) on the grid is inconsequential, the aggregated effect of a large number of PEVs poses challenges to the existing grid. As a consequence, identification of their impact and smart-charging techniques needs to be developed.

A number of research works have been carried out to analyze the impact of EV charging on the distribution network. Till date, optimal PEV charging schemes have focused on two objectives. The first aims to provide utility-level benefits of ancillary services by shifting the EV load to off-peak load hours. The other aims at maximizing the EV owners'

benefit by reducing the overall charging cost of the PEVs. However, both approaches have certain limitations. The techniques focusing on utility benefits neglect EV owner preferences and benefits, while customer-centric strategies do not consider the impact of utilizing a Time of Use (TOU)-based tariff, which may introduce a secondary peak due to PEV charging loads. Despite the large number of techniques proposed for EV charging, no scheme aims to simultaneously reduce the cost of charging and voltage variability in the system.

This work builds a framework to provide an optimal charging schedule that minimizes the overall charging cost of the PEVs as well as voltage variability in the network while taking electricity price fluctuations into account. The proposed scheme considers the simultaneous minimization of charging costs of all the EVs along with the deviation of bus voltages from the desired values. For this, a multi-objective function has been proposed that has been optimized under a set of operating constraints. A Linear Programming (LP) approach is employed in a distribution system with instantaneous load and PEVs to compute the voltage at each node. The problem is formulated wherein the instantaneous load and electricity tariff is known in advance. The optimization technique provides a re-distribution of the PEV charging load while fulfilling the whole set of constraints. A real-time simulation and validation of the proposed approach are carried out on a Real-Time Digital Simulator (RTDS) and Real-Time Automation Controller (RTAC) platform to reaffirm the efficacy and feasibility.

3.2 TEST SYSTEM MODELLING

An eight-node radial distribution system shown in Fig. 3.1 is considered for testing the proposed methodology. In the figure, nodes with PEV connection have been marked with a black "dot". Two test systems are considered, with the line parameters of both the

considered test systems are shown in Table 3.1. Test System I, as well as Test System II, are represented by an eight-node radial distribution network shown in Fig. 3.1. However, two of the lines of Test System II have higher lengths compared to Test System I. This has resulted in increased resistance and reactance of these lines. Each line of the two test systems employs a standard low-voltage cable with an impedance of $0.446 + j0.071\ \Omega/km$ [95]. It is observed from Table 3.1. that lines between buses 4-5 and 7-8 of Test System II have higher lengths compared to Test System I. The increase in line length causes voltage deteriorations at a few nodes due to the increase in the line voltage drop.

An individual aggregator controls the entire distribution system. It is assumed that upon arrival, every PEV owner shares the PEV information, i.e., battery capacity, current State of Charge (SOC), desired SOC, and parking time, with the aggregator. Each PEV owner is in agreement with the aggregator on tariff structure and PEV consumption/injection daily requirements.

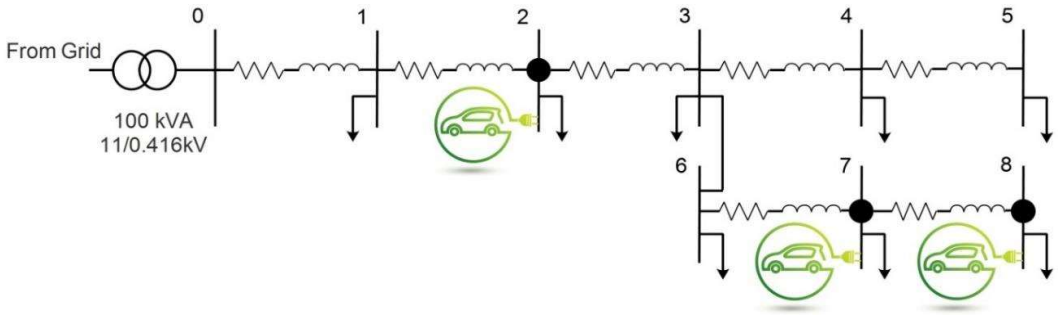

Fig. 3.1 Single-line diagram of the test system.

Table 3.1 Test system line parameters ($0.446 + j0.071\Omega/km$).

Line		Test System I			Test System II		
From Bus	To Bus	Line Length (m)	R(Ω)	X(Ω)	Line Length (m)	R(Ω)	X(Ω)
0	1	115	0.0513	0.008	115	0.0513	0.008
1	2	115	0.0513	0.008	115	0.0513	0.008
2	3	230.2	0.1027	0.016	230.2	0.1027	0.016
3	4	345.3	0.1540	0.024	345.3	0.1540	0.024
4	5	345.3	0.1540	0.024	575.3	0.2566	0.041
3	6	230.2	0.1027	0.016	230.2	0.1027	0.016
6	7	115	0.0513	0.008	115	0.0513	0.008
7	8	230.2	0.1027	0.016	345.3	0.1540	0.024

3.3 PROBLEM FORMULATION

The objective of the proposed scheme is to minimize the recharging cost of the total number of PEVs and bus voltage variations while considering the constraints on charging/discharging rates, SOC limits, and voltage tolerance on each node. The entire time period T is divided evenly into K discrete time steps such that $K = T/\tau$, where τ is the duration of each time step (considered 30 min in our case). The objective function for minimization of the charging cost of PEVs is defined as:

$$min \sum_{k=1}^{K} \sum_{n=1}^{N} s_k C_k \tau X_k^n \tag{3.1}$$

where the charging cost in k^{th} time interval, C_k is in $\$/kWh$, and the charging/discharging rate of n^{th} PEV in k^{th} time interval, X_k^n is in kW with N

representing the total number of PEVs present in the system. A binary variable s_k is chosen to denote the charging status of the connected PEV in k^{th} time interval as:

$$s_k \in \{0,1\}, \forall k = \{1,2, \dots, K\} \tag{3.2}$$

The charging cost represented by equation (3.1) is optimized using the technique presented in Section 2.1 (Chapter 2) in TOU-based tariff structure with price per kWh of energy consumed in the off-peak price period, i.e., $c_{off-peak} = 0.092\ \$/kWh$ and price per kWh of energy consumed in peak price hours given by equation (2.18).

The second objective of the scheme aims to minimize the voltage variability in the system by utilizing the PEV charging/discharging rates. The voltage variability in the system can be defined as the sum of the deviations of the node voltage from the nominal value. The mathematical formulation for calculating voltage variability over the entire time period is as follows:

$$V_{var} = \sum_{k=1}^{K} \sum_{n=1}^{N} 1 - V_n(k, X_k^n, SOC_k^n) \tag{3.3}$$

where, V_n is the voltage of the node supplying n^{th}PEV.

Here, V_{var} is the cost function to be minimized with the SOC, SOC_k^n as the state variable evolves as per the control variable, the charging rate of the PEV X_k^n. To recapitulate, the overall objective function is formulated as follows:

$$\min f_0(\overline{X}) = \sum_{k=1}^{K} \sum_{n=1}^{N} s_k C_k \tau X_k^n + \sum_{k=1}^{K} \sum_{n=1}^{N} 1 - V_n(k, X_k^n, SOC_k^n) \tag{3.4}$$

$$\text{where, } \overline{X} = \{X_k^n, V_n^k\}, \forall n = \{1,2, \dots, N\}, \forall k = \{1,2, \dots, K\}$$

The above-formulated objective is subjected to the following constraints:

3.3.1 Charging rate constraints

The PEV chargers having bi-directional power flow capability have limitations over their charging/discharging rate. For each PEV, this limitation is imposed as:

$$-X^{n,min} \leq X_k^n \leq X^{n,max}, \forall n = \{1,2,\dots,N\}, \forall k = \{1,2,\dots,K\} \quad (3.5)$$

where X^n is the nominal charging power of the n^{th} PEV charger in kW.

3.3.2 Constraints on the state of charge

Two-level constraints are imposed on the state of charge. The battery state of charge of n^{th} PEV at the end of k^{th} time interval is given by,

$$SOC_k^n = SOC_0^n + \tau \sum_{k=1}^{K} s_k X_k^n, \forall n = \{1,2,\dots,N\}, \forall k = \{1,2,\dots,K\} \quad (3.6)$$

where, SOC_0^n is the initial state of charge of the PEV battery in kWh.

To maintain the battery health, it is implicated to avoid overcharging and hence, a restriction is imposed on the state of charge at every time step,

$$SOC_k^{n,min} \leq SOC_k^n \leq SOC_k^{n,max}, \forall n = \{1,2,\dots,N\}, \forall k = \{1,2,\dots,K\} \quad (3.7)$$

where, $SOC_k^{n,min}$ and $SOC_k^{n,max}$ are the minimum and maximum permissible limits on the state of charge of the PEV battery.

On the other hand, a hard constraint, i.e., the desired state of charge SOC_d^n is imposed by the respective PEV owner. This is given by,

$$SOC_d^n = SOC_0^n + \tau \sum_{k=1}^{K} s_k X_k^n, \forall k = \{1,2,\dots,K\} \quad (3.8)$$

3.3.3 Power flow balance constraint

The active power balance in the network with the inclusion of EVs is represented in the form of equality constraint as:

$$P_k = P_{k,base\ load} + \sum_{n=1}^{N} s_k X_k^n, \forall n = \{1,2,\dots,N\}, \forall k = \{1,2,\dots,K\} \quad (3.9)$$

where, P_k is the total power drawn from the grid in the k^{th} time interval, $P_{k,base\ load}$ is the power drawn by the non-EV loads in the k^{th} time interval and $\sum_{n=1}^{N} s_k X_k^n$ is the cumulative power of all the plugged-in EVs in the k^{th} time interval. The charging/discharging rate, X_k^n is positive while PEV is charging and negative while discharging. Thus, PEV acts as a load while charging and drawing power from the grid, whereas it acts as a source while discharging the available power into the grid.

3.3.4 Voltage level constraints

In this work, a low voltage distribution system is considered with voltage V_k^j, at j^{th} bus in k^{th} time interval of the day for 24 hours.

$$V_{min}^j \leq V_k^j \leq V_{max}^j, \forall j = \{1,2,\dots,J\}, \forall k = \{1,2,\dots,K\} \quad (3.10)$$

where, V_{min}^j and V_{max}^j represents the minimum, and maximum permissible voltages at j^{th} bus, and J is the total number of buses present in the system. In this work, the permissible voltage variation has been considered $\pm 10\%$ at all the buses. The above-formulated problem is solved using Interior-Point Method (IPM), i.e., Newton's method for equality constraints and the Barrier method presented in Section 2.2 (Chapter 2).

3.4 CASE STUDY

The base case system voltage profile for 24h [96] for Test System I (voltage profile of Test System I under uncoordinated charging) is shown in Fig. 3.2. The 24h load multiplier factor is shown in Fig. 3.3, which represents the load variations for the 24h period considered in this work. The 24h time scale shows the actual time of the day, starting from 01:30 P.M. (13.5h) of day 1 to 01:30 P.M. (13.5h) of day 2.

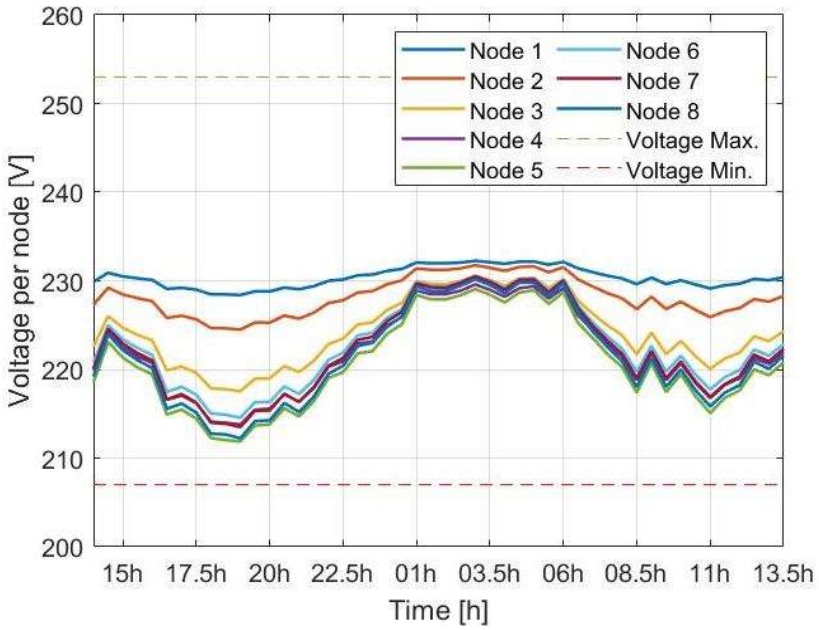

Fig. 3.2 Voltage profile of the system in Case I.

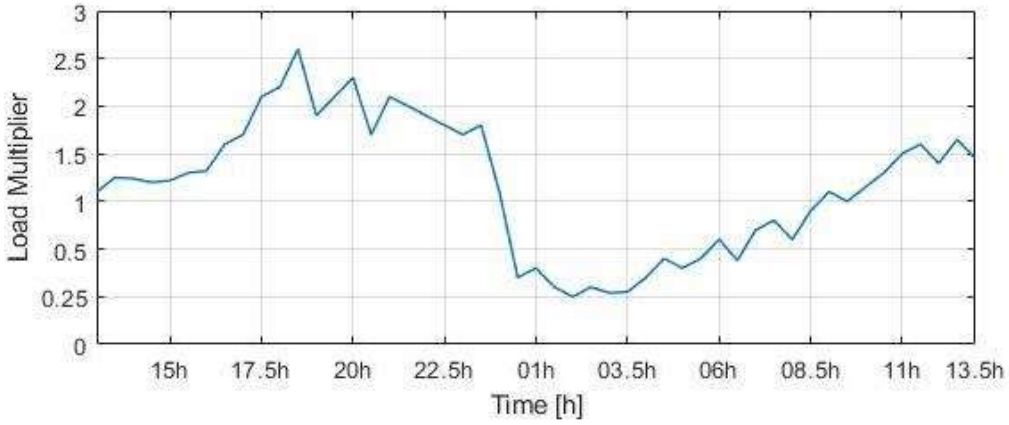

Fig. 3.3 Load multiplier factor for 24h period.

The secondary voltage of the transformer node is fixed at 230V. The charging/discharging rate of PEVs is limited to 3 kW/h to imitate Level-I slow charging, while the nominal battery capacity of the PEV is 30 kWh. However, only 90% (27 kWh) of the capacity is utilized to maintain the battery life. The charging profile of all the PEVs is consistent with the connection period from 5 P.M. (17:00h) to 6 A.M. (06:00h). It is assumed that all the EVs arriving for charging have a certain SOC left. In this work, we have considered 25%, 50% and 75% SOC for PEV#1, PEV#2 and PEV#3 to represent the different SOC conditions for three EVs. The tariff structure for a continuous portion of 24h is shown in Fig. 3.4.

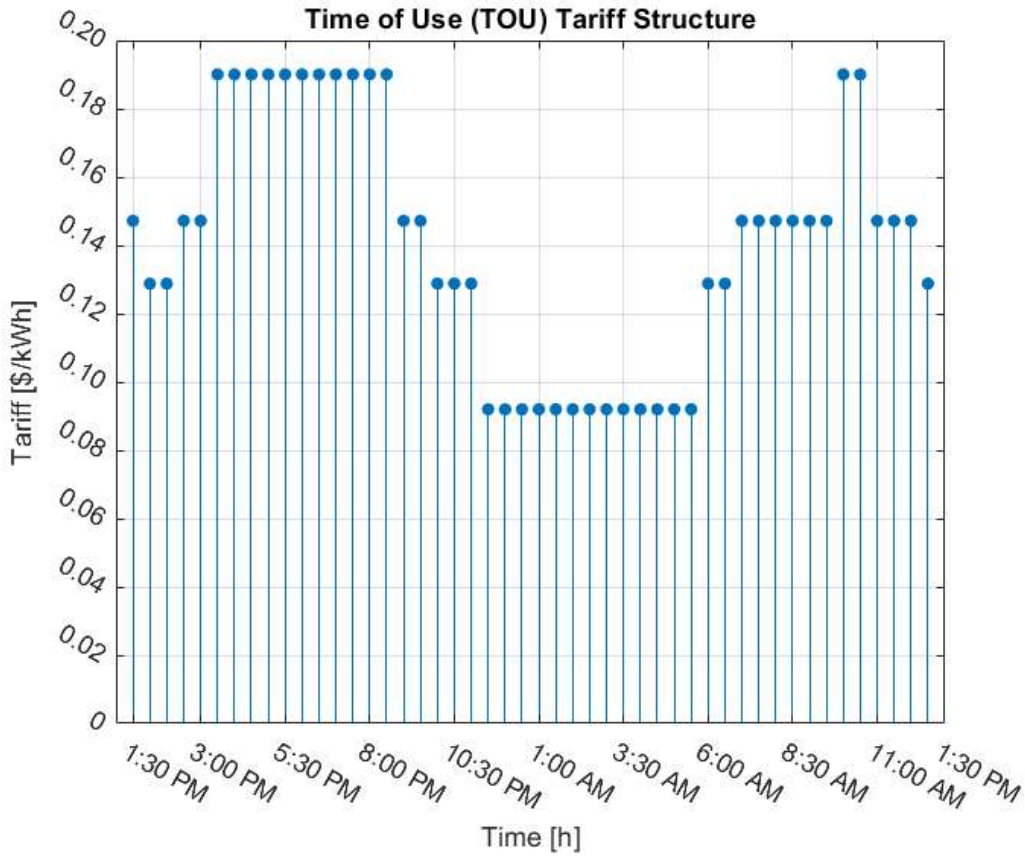

Fig. 3.4 TOU-based tariff structure.

Multiple case scenarios are simulated on the adopted test systems. In Test System I, the load profile does not cause a violation of the voltage limits. The voltages at each node are within the permissible range of 0.9 p.u. (207 V) to 1.1 p.u. (253 V). While in Test System

II, a slight variation in the line parameters causes a violation of voltage limits on Nodes #5, #6, #7, and #8 at specific instants of peak load.

In the case of un-coordinated charging of PEVs, each vehicle draws power at a maximum charging rate, i.e., 3 kW/h in our case, up to the SOC desired by the PEV owner, as presented below:

PEV#1: 75% charging in 6.75h, i.e., 5 P.M. to 11:45 P.M.

PEV#2: 50% charging in 4.5h, i.e., 5 P.M. to 9:30 P.M.

PEV#3: 25% charging in 2.25h, i.e., 5 P.M. to 7:15 P.M.

It is noteworthy to mention that all the PEVs are charging during the peak load hours, and hence, causes a significant voltage drop in the already burdened system. The energy consumption of the PEVs for the above-described periods for all the PEVs, as shown in TOU based tariff shown in Fig. 3.4, are:

PEV#1: Energy consumed from 5 P.M. to 10 P.M. at the rate of $0.19\ \$/kWh$, 10 P.M. to 11 P.M. at the rate of $0.15\ \$/kWh$, and during 11 P.M. to 11:45 P.M. at $0.13\ \$/kWh$.

PEV#2: Energy consumed from 5 P.M. to 9:30 P.M. at the rate of $0.19\ \$/kWh$.

PEV#3: Energy consumed from 5 P.M. to 7:15 P.M. at the rate of $0.19\ \$/kWh$.

The overall charging cost in TOU based scenario for the PEVs in the case of un-coordinated charging for Test System I is $3\times(5 \times 0.19 + 1 \times 0.15 + 0.75 \times 0.13 + 4.5 \times 0.19 + 2.25 \times 0.19) = \$7.44$.

The overall charging cost in TOU based scenario for the PEVs in the case of un-coordinated charging for Test System II is calculated to be $\$7.71$.

3.4.1 Case I: Voltage profiles within tolerance limits (Test System I)

The proposed optimization technique is applied to the first test system. The plot of variations of SOC, charging/discharging profiles of three PEVs, node (bus) voltages under PEVs charging, system loading with and without PEVs, against time for 24 hours period considered are shown in Fig. 3.5 (a), Fig. 3.5 (b), Fig. 3.5 (c) and Fig. 3.5 (d), respectively. It is observed from Fig. 3.5 (c) that all node voltages are within permissible limits under PEVs charging/discharging in Test System I. It is observed from Fig. 3.5 (d) that the original load profile is re-distributed while the EVs are plugged in. It is noteworthy to mention that the entire charging load of PEVs is shifted to the periods of off-peak load. It is observed from Fig. 3.5 (b) that the PEVs inject power into the system during peak load hours as per the available SOC. Thus, PEVs try to flatten the voltage profile during the entire charging period. The SOC characteristics in Fig. 3.5 (a) show that all the PEVs are charged up to the desired SOC by the departure time.

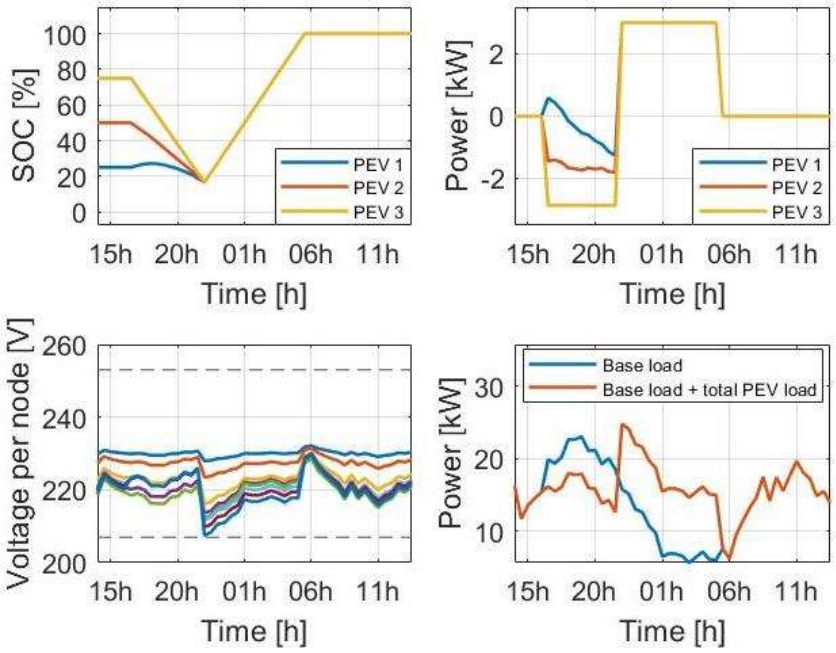

Fig. 3.5 Case I (a) SOC profiles of PEVs battery, (b) Charging/Discharging profile of PEVs, (c) Voltage profile of the system, and (d) Load profile of the system.

The 3-D bar plot in Fig. 3.6 shows the cost of charging all three PEVs in the TOU-based tariff scenario. The cost incurred to the PEV owner while charging/discharging the vehicle on a half-hourly basis is taken on the z-axis and represented by the colour bar. Each bar corresponding to the specific PEV and time interval represents incurred cost. The overall charging cost of all three PEVs in this schedule is $2.07. In this case, PEVs inject power into the system during peak load hours. It is to be noted that the prosumers (PEV owners) are penalized while charging during peak hours. Thus, PEV owners prefer to charge during off-peak hours and discharge during peak hours to earn benefits from the TOU-based tariff structure.

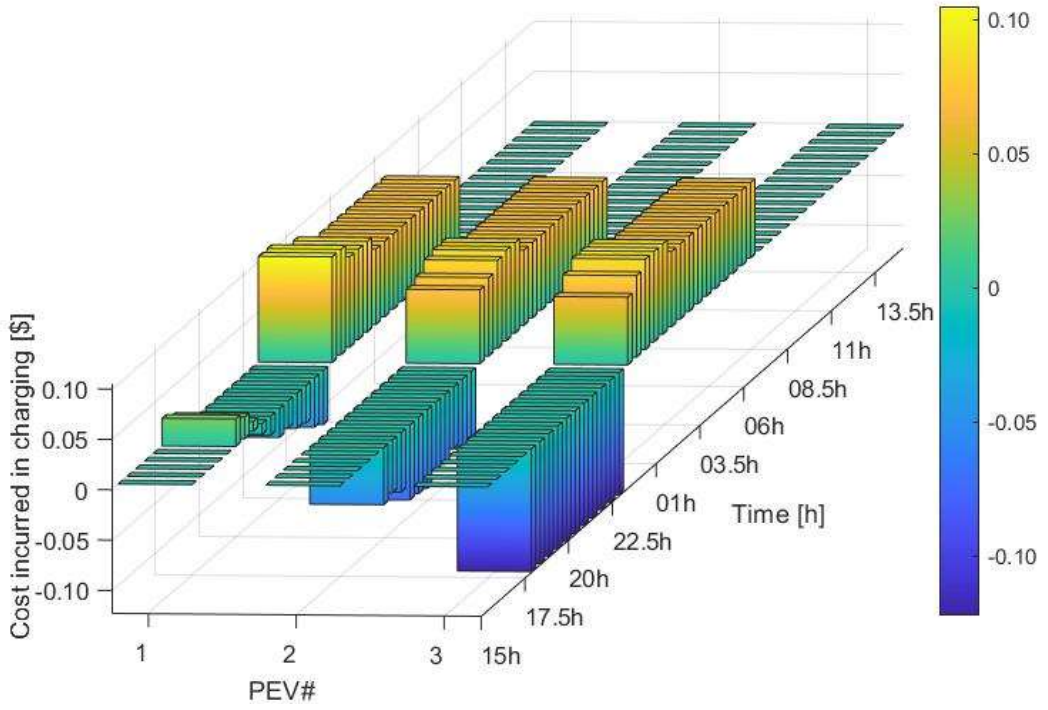

Fig. 3.6 Cost of charging of PEVs for Case I.

3.4.2 Case II: Voltage profiles violating tolerance limits (Test System II)

Case II corresponds to investigations carried out on Test System II. In this test case, the voltage at specific nodes (Nodes #5, #6, #7, and #8) violate the lower limit of voltage tolerance even without PEVs, as shown in Fig. 3.7. To demonstrate the effectiveness of the proposed scheme, the EVs are plugged in during peak load hours. If the PEVs do not have enough initial SOC, they cannot inject sufficient power into the system to respect voltage constraints. In this scenario, no feasible solution can be achieved.

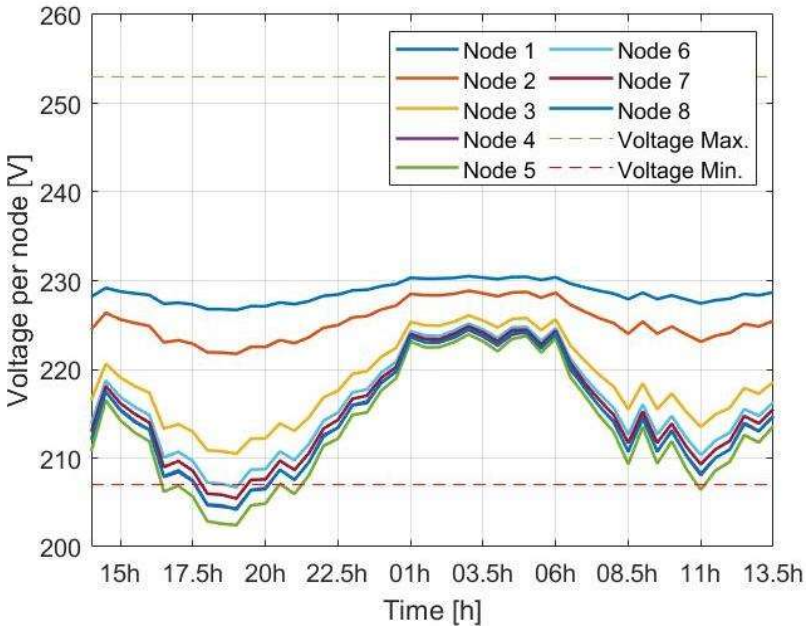

Fig. 3.7 Voltage profile of the system in the absence of PEVs Case II.

After applying the proposed optimization technique, if the PEVs have sufficient initial SOC, they discharge into the system and compensate for the peak load. The variations of SOC of PEVs, charging/discharging of PEVs, node voltages in the presence of PEVs, and system loading with and without PEVs, against time for 24 hours period considered are shown in Fig. 3.8 (a), Fig. 3.8 (b), Fig. 3.8 (c), and Fig. 3.8 (d), respectively. It can be noticed from Fig. 3.8 (c) that all the node voltages are now satisfying the voltage constraints during the connection periods of PEVs (17:00h to 06:00h). It is seen that the voltage at Node#5 at 11h is violating the security limits, and the excess load cannot be compensated due to the unavailability of PEVs. Fig. 3.8 (b) shows the charging profiles of each of the PEVs. The re-distribution of the entire charging load can be easily observed. During this re-distribution, PEVs with initial SOC discharge into the system during peak load period to make the maximum profit as the electricity charges are high. At 17h, PEV#1, with 25% of initial SOC, slightly charges its battery, while PEV#2 and

PEV#3 start selling their energy during peak price hours. Later all three PEVs charge their batteries in low price hours and charge up to desired SOC by departure time.

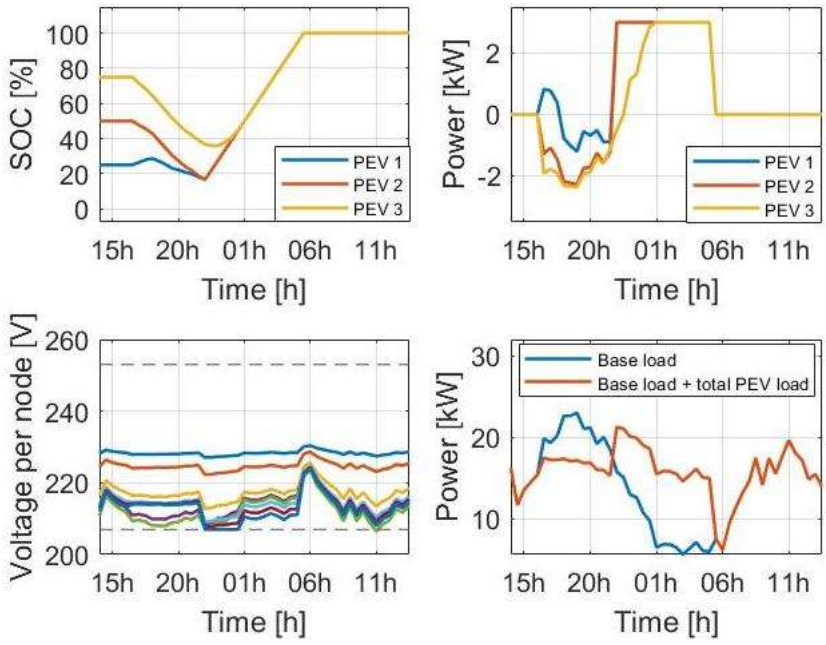

Fig. 3.8 Case II (a) SOC profiles of PEVs battery, (b) Charging/Discharging profile of PEVs, (c) Voltage profile of the system, and (d) Load profile of the system.

The optimal charging cost of all the PEVs for the entire charging duration is shown in Fig. 3.9. The overall charging cost of the PEVs is calculated to be $2.35.

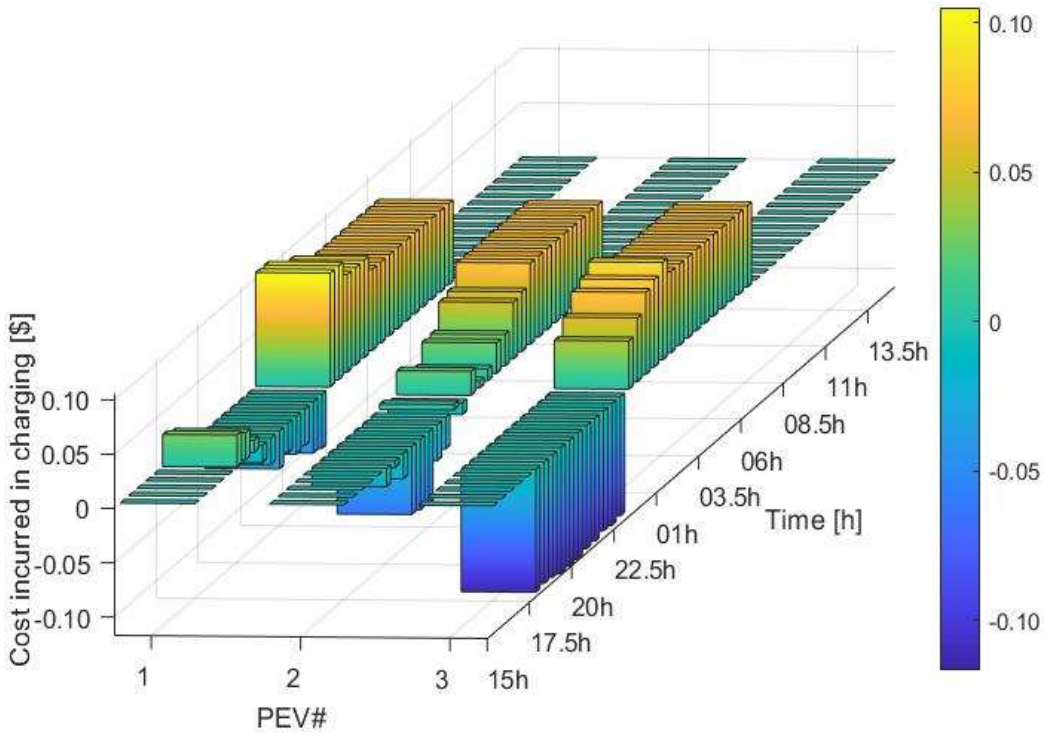

Fig. 3.9 Cost of charging of PEVs for Case II.

3.4.3 Case III: PEVs initial SOC near battery capacity for both the Test Systems

This case is simulated to demonstrate the capabilities of PEVs from the owner's perspective. In this case, each of the PEVs has initial SOC near their battery capacity. It is assumed that the PEVs were not on a trip or were on a very short trip since the last recharge. The initial SOC of PEVs are supposed to be:

PEV#1: 75% of the battery capacity, i.e., 20.25kWh

PEV#2: 75% of the battery capacity, i.e., 20.25kWh

PEV#3: 100% of the battery capacity, i.e., 27kWh

This scenario is simulated on both test systems. In the case of the first test system, all the node voltages respect the voltage tolerance limits in the absence of PEVs, as presented

earlier. The variations of SOC of PEVs, charging/discharging of PEVs, node voltages in the presence of PEVs, and system loading with and without PEVs, against time for 24 hours period considered are shown in Fig. 3.10 (a), Fig. 3.10 (b), Fig. 3.10 (c), and Fig. 3.10 (d), respectively. Since the PEVs are intensely charged, they try to sell the energy during high-price periods, as observed from Fig. 3.10 (a) and (b). During the PEVs charging time frame, the voltages of all the nodes lie within the tolerance limits, as shown in Fig. 3.10 (c).

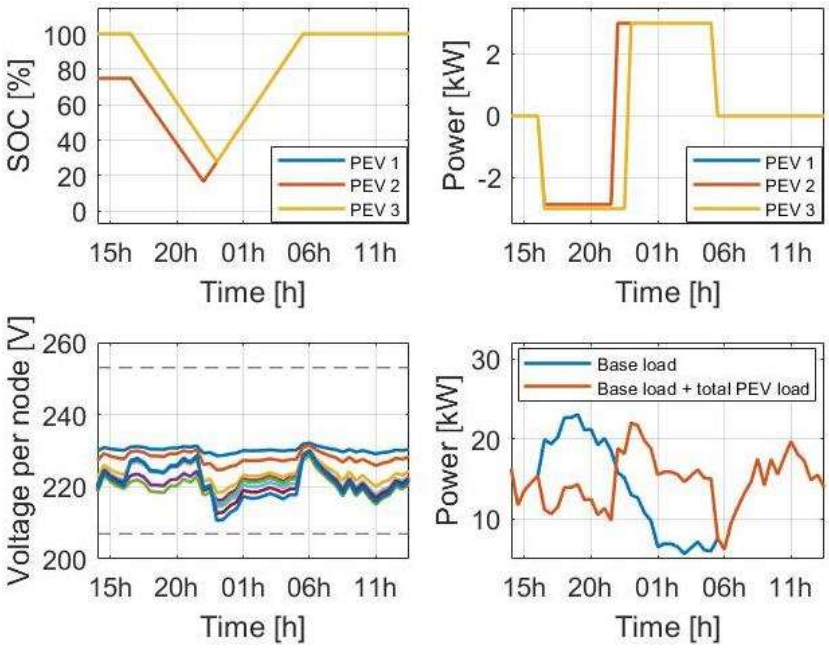

Fig. 3.10 Case III, Test System I (a) SOC profiles of PEVs battery, (b) Charging/Discharging profile of PEVs, (c) Voltage profile of the system, and (d) Load profile of the system.

It is essential to highlight that the charging cost of the PEVs in this scenario is $-2.80, as shown in Fig. 3.11. The negative charging cost indicates that the PEV owners profit from the recharging schedule in this scenario. It is implicit from the wide range of charging times available with the PEVs that if the PEVs have initial surplus energy, they can exploit the TOU-based tariff structure.

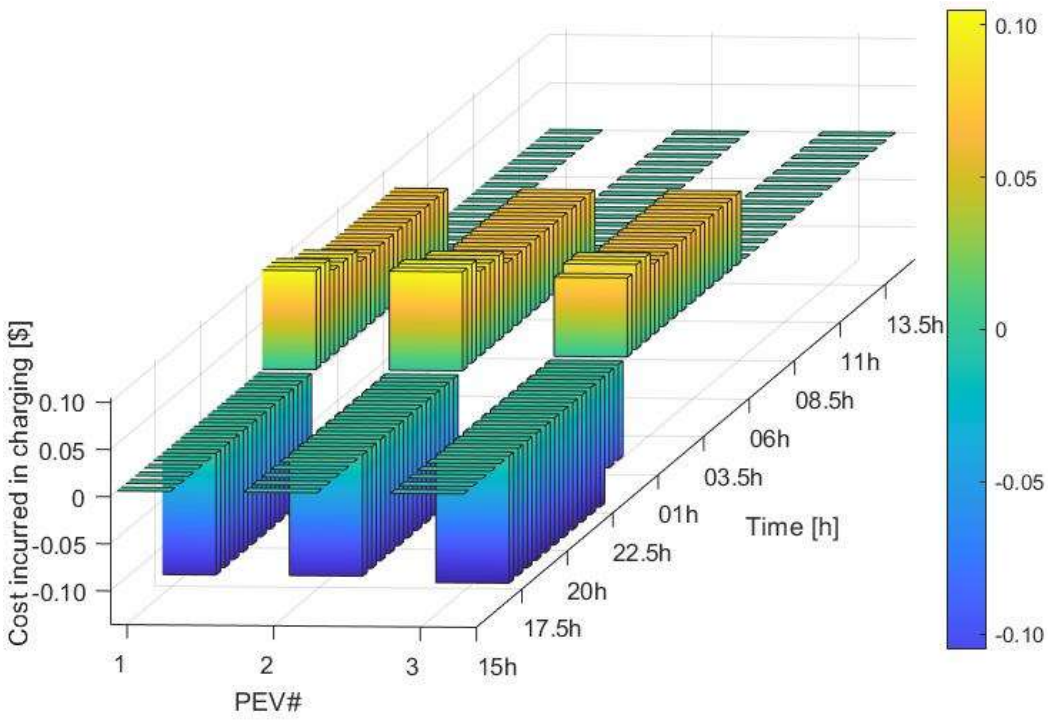

Fig. 3.11 Cost of charging of PEVs for Case III (Test System I).

In the second test system, the voltages at specific nodes violate security limits even without PEVs, as shown in Fig. 3.12. Few nodes at specific time instants are marked as data tips in the figure. Node#5, with the highest loading, has the largest voltage drop during a significant period. i.e. 16-21h.

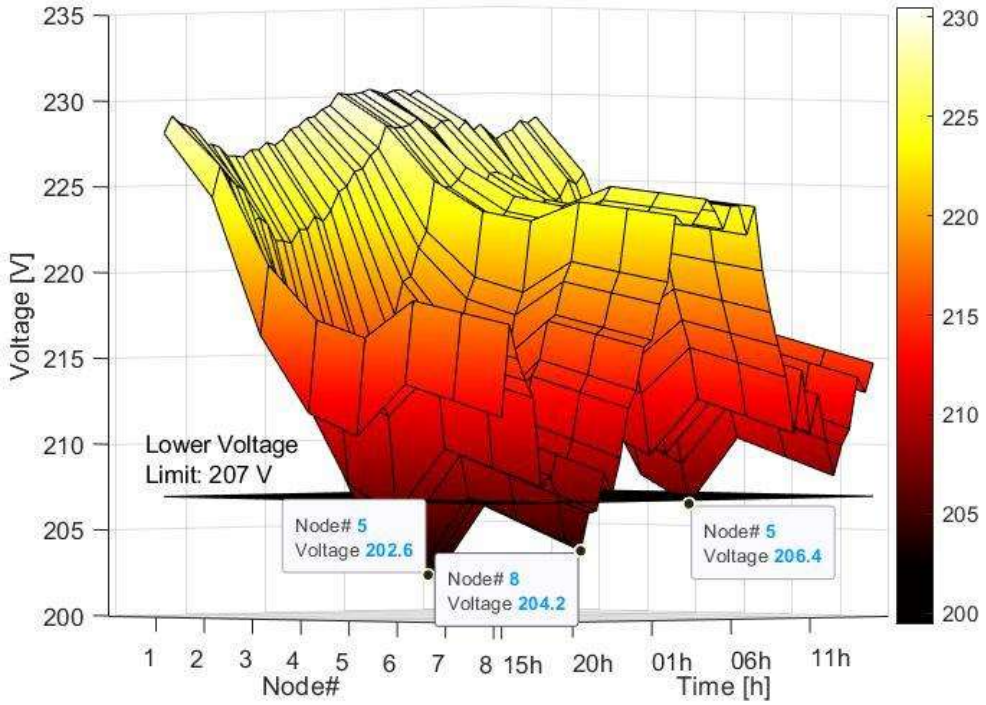

Fig. 3.12 Voltage profile (surface plot) of the system for Case III (Test System II).

The variations of SOC of PEVs, charging/discharging of PEVs, node voltages in the presence of PEVs, and system loading with and without PEVs, against time for 24 hours period considered are shown in Fig. 3.13 (a), Fig. 3.13 (b), Fig. 3.13 (c), and Fig. 3.13 (d), respectively. The node voltage variations against time in the presence of PEVs are shown in Fig. 3.14. After applying the optimization technique, PEVs with sufficient SOC bring the voltages to the permissible limits during the charging time frame, as shown in Fig. 3.13 (a). It is observed from Fig. 3.14 that voltage at Node#5 around 11h falls below the lower permissible limit. This is justified as the PEVs providing voltage support had departed already by that time as departure time is assumed to be 06hr for all the PEVs.

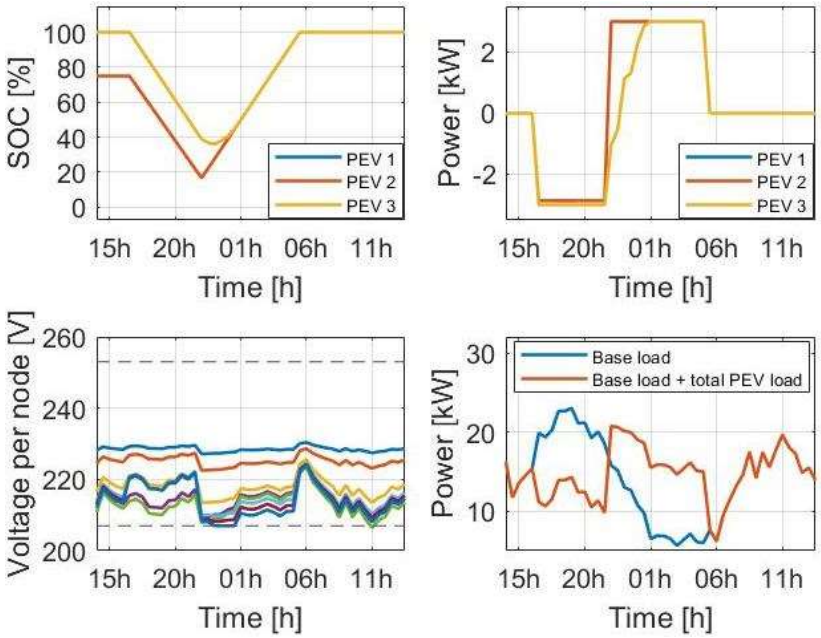

Fig. 3.13 Case III, Test System II (a) SOC profiles of PEVs battery, (b) Charging/Discharging profile of PEVs, (c) Voltage profile of the system, and (d) Load profile of the system.

The charging cost of the entire schedule is calculated to be $-2.76 (Fig. 3.15). The profit of PEV owners is slightly less in this case as compared to $-2.80 for the first test system. This is since PEV#3 does not deeply discharge into the system, i.e., till 8kWh of SOC as in the first case, as seen from Fig. 3.13 (b). PEV#3 is connected at Node#8, which is heavily loaded. Even after the rescheduling of the entire charging load, the voltage at Node#8 is near the lower tolerance limits. Recharging the battery at the maximum rate to reach the desired SOC in the available charging time frame, i.e., 18kW in 8h, may bring the voltage at Node#8 below the tolerance limit. Hence, PEV#3 charges at a rate below 3kW/h till the voltage at Node#8 is well above the lower tolerance limit.

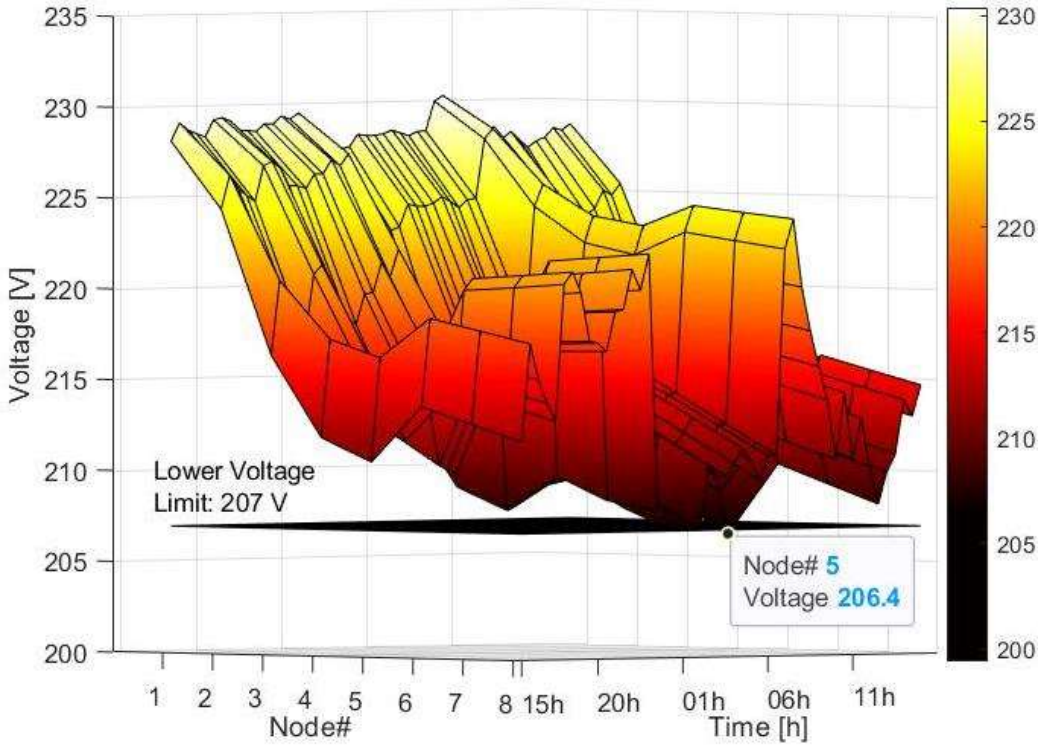

Fig. 3.14 Voltage profile (surface plot) of the system after PEVs voltage support for Case III (Test System II).

So, it is important to highlight from the above discussion that the profit-making depends not only on tariff structure, nominal charging/discharging rate, available time of connected PEV before departure and initial SOC but also upon the location of the connected PEV.

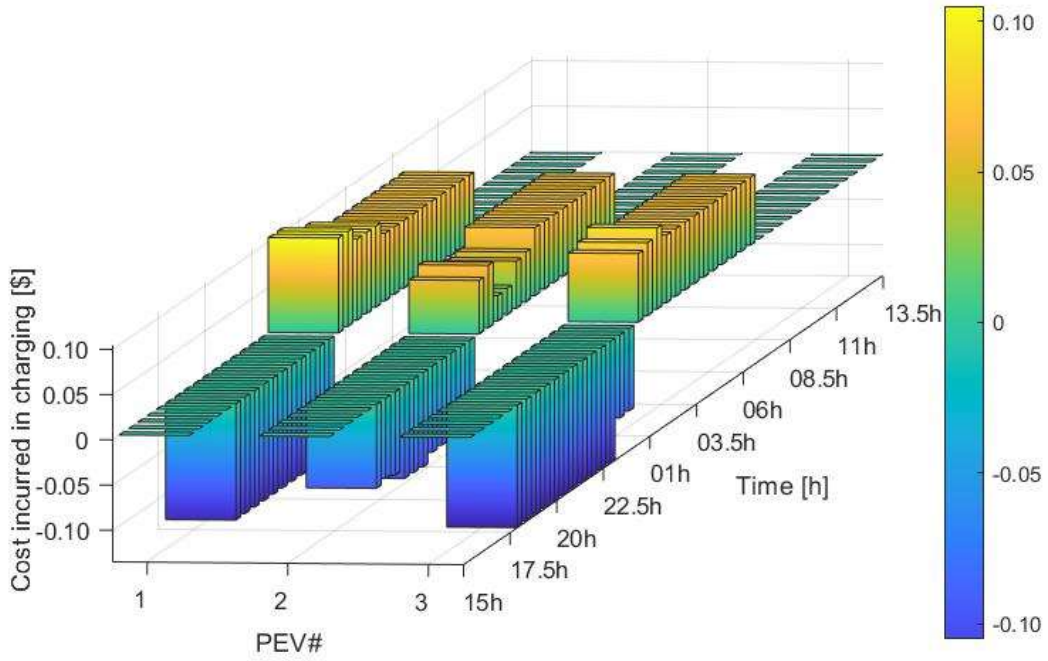

Fig. 3.15 Cost of charging of PEVs for Case III (Test System II).

The comparison between the reduction in charging cost of the PEVs and reduction in voltage variability in the system in the case of optimal charging in TOU-based tariff for all the simulated cases is inked in Table 3.2. It is observed from Table 3.2 that the optimal scheduling of PEVs shifts the charging load to off-peak load hours, thereby improving the system voltages apart from charging cost reduction for all the cases.

Table 3.2 Comparison of charging cost of PEVs and voltage variability in different simulated cases.

Parameters	Un-coordinated PEV charging		Proposed PEV Charging Scheme			
			Case I: Base case voltage profile within tolerance limits	Case II: Base case voltage profile violating tolerance limits	Case III: PEVs initial SOC near battery capacity	
	Test System I	Test System II	Test System I	Test System II	Test System I	Test System II
Min. System Voltage without PEVs	211.9 V	202 V	211.9 V	202 V	211.9 V	202 V
Min. System Voltage with PEVs in TOU-based Tariff	197.6 V	191 V	207.5 V	207 V	211 V	207 V
Cost of the overall Charging/Discharging Schedule	$7.44	$7.71	$2.07	$2.35	$-2.80	$-2.76
Reduction in Charging Cost from Un-coordinated Charging	-	-	72.02 %	68.38 %	209.32 %	207.66 %
Reduction in Voltage Variability	-	-	5.34 %	5.6 %	1.74 %	1.9 %

"–" Not Applicable

3.5 VALIDATION OF THE PROPOSED SCHEME ON A REAL-TIME DIGITAL SIMULATOR (RTDS) PLATFORM

The efficacy of the proposed methodology is evaluated in real-time by realizing it in a Real-Time Digital Simulator. A practical IEEE 34-node test system with a rated line voltage of 24.9kV (rated phase voltage of 14.4kV) and 60Hz system frequency [97], as shown in Fig. 3.16, is chosen and modelled in the RSCAD environment. The simulator comprising a NovaCor with four licensed cores, a GTNETx2 card and RSCAD FX 1.2 software is used in this work. The simulation is carried out in distribution mode with a simulation time step of 150.0µs. The schematic of the test system for real-time implementation is inked in Fig. 3.17.

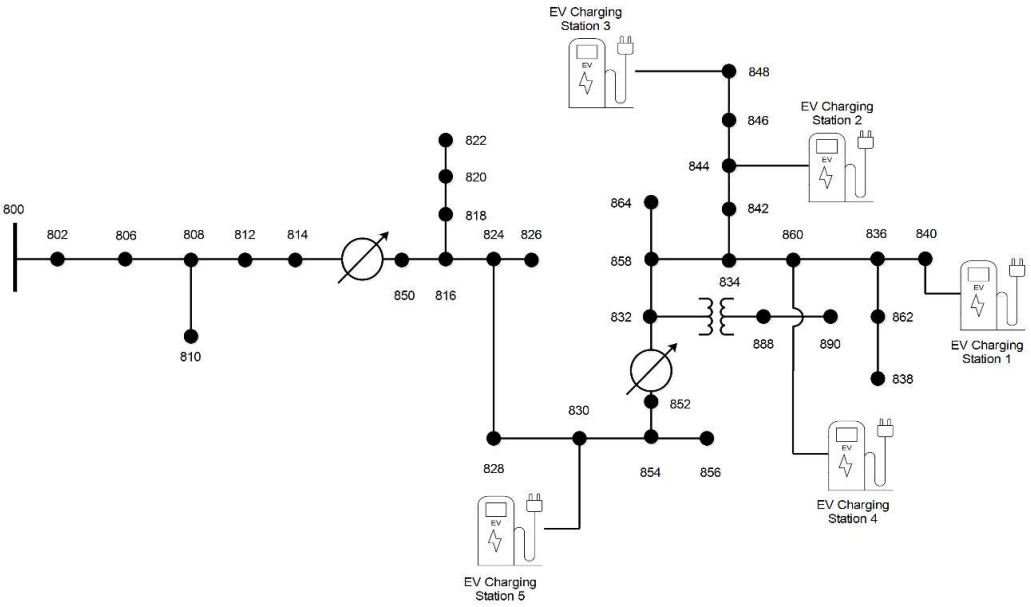

Fig. 3.16 IEEE 34-node test feeder with EV charging stations.

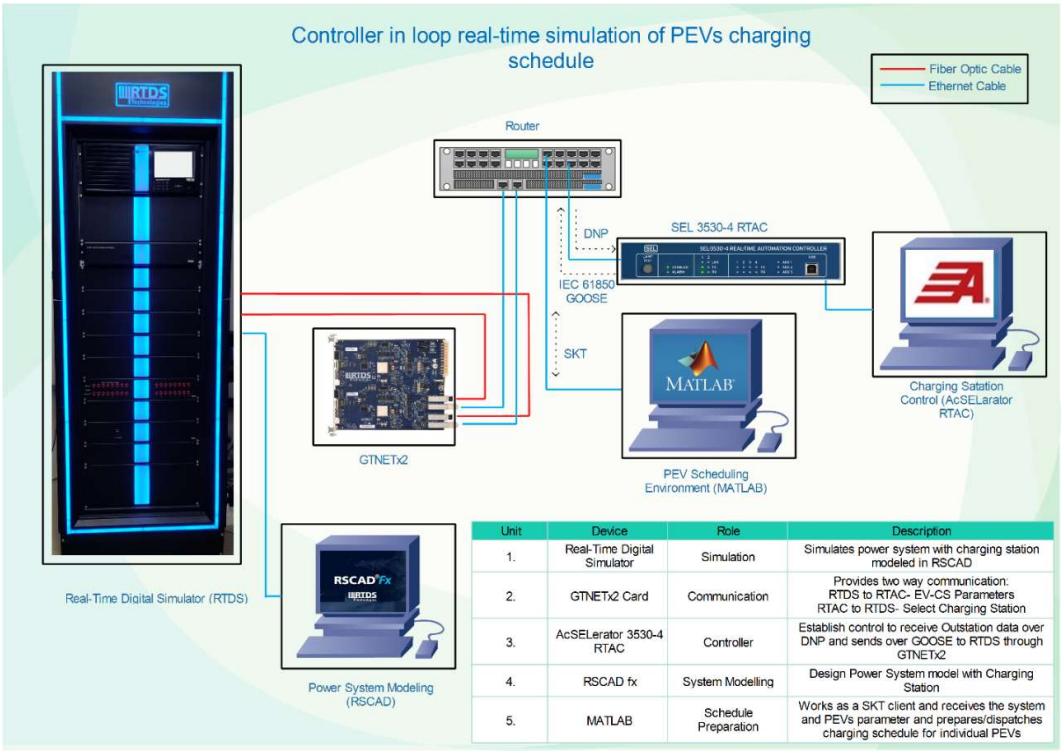

Unit	Device	Role	Description
1.	Real-Time Digital Simulator	Simulation	Simulates power system with charging station modeled in RSCAD
2.	GTNETx2 Card	Communication	Provides two way communication: RTDS to RTAC- EV-CS Parameters RTAC to RTDS- Select Charging Station
3.	AcSELerator 3530-4 RTAC	Controller	Establish control to receive Outstation data over DNP and sends over GOOSE to RTDS through GTNETx2
4.	RSCAD fx	System Modelling	Design Power System model with Charging Station
5.	MATLAB	Schedule Preparation	Works as a SKT client and receives the system and PEVs parameter and prepares/dispatches charging schedule for individual PEVs

Fig. 3.17 Controller Hardware In Loop (CHIL) simulation of PEVs charging schedule with Real-Time Digital Simulator.

In the test system, five charging stations are placed on nodes 840, 844, 848, 860 and 830. Under intermediary load conditions, 1640kW load can be increased without reaching the node voltage limit, which is equivalent to 854 PEVs with Level 1 charging (Slow Charging at 1.92kW) or 227 PEVs with Level 2 charging (Fast Charging at 7.2kW) [98]. To imitate the EVs specification, the EV parameters in the RSCAD draft are selected as follows:

Level 1: 480EVs with Level 1 charging (with an aggregated charging power of 921.6kW)

Level 2: 100EVs with Level 2 charging (with an aggregated charging power of 720kW)

The battery capacity of the EVs with Level 1 and 2 charging is selected as 30.2kWh [99] and 76.4kWh [100], respectively. EVs battery range depends upon the daily driving pattern, battery type and capacity. To address this uncertainty, the initial SOC of all the EVs upon arrival is generated through a randomize function. For every simulated case,

this function generates a random value (within the PEVs battery SOC limits) for the initial SOC of the arriving EV.

To address the communication feasibility for the external application (MATLAB), industry-standard protocol, i.e., Socket Protocol (SKT), is utilized to establish communication between RTDS and MATLAB. The Transmission Control Protocol/Information Protocol (TCP/IP) based communication is established with RTDS as the TCP server and MATLAB as a client. The Application Programming Interface (API) call initiates the handshaking from the client 'connect()', and data exchange starts between the server and the client. The system variable signals, node voltages, EVs arrival and indicated departure time, initial and desired SOC, and nominal charging and discharging rates are sent by the TCP server and EVs charging schedule is prepared by the client and dispatched to the server. On the arrival of a new EV, the signals are again sent to the TCP client, and the charging schedule for only new EVs is prepared and dispatched.

In the testbed shown in Fig. 3.17, the Distributed Network Protocol 3 (DNP3) master is established in the GTNETx2 card of RTDS while the slave resides in RTAC. The signals sent from the runtime simulation to SEL 3530-4 RTAC outstation over DNP3 are charging station voltages and frequency with the limiting parameters, as shown in Table 3.3.

Table 3.3 Charging station Voltage (V) and Frequency (f) check.

Description	**Value**
Maximum Voltage Limit	1.1p.u.
Minimum Voltage Limit	0.9p.u.
Maximum frequency Limit	1.01p.u.
Minimum frequency Limit	0.99p.u.
Drop-off time for V/f check	0.5 sec

Once the connection is successfully established between RTDS GTNETx2 and RTAC, the packet count in the DNP3 controller is shown in Fig. 3.18. The total number of messages sent is 104, while the number of messages received is 54. The total successful message count is 158, with 0 message failures denoting the reliability of the connection between the two devices.

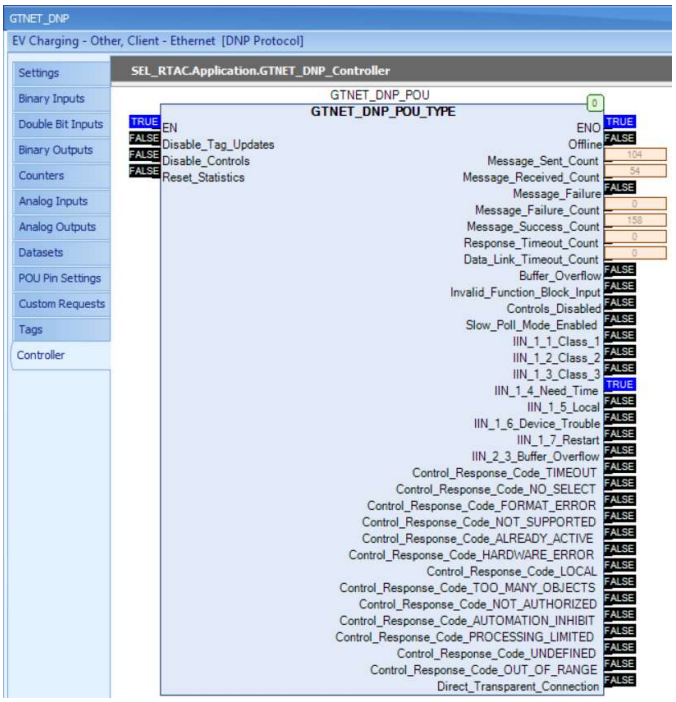

Fig. 3.18 DNP3 controller in SEL AcSELerator RTAC.

In an automated system, IEC-61850, Generic Object Oriented System-Wide Events (GOOSE) messaging is an event-triggered communication between Intelligent Electronic Devices (IEDs). Here RTAC behaves as a GOOSE publisher and GTNETx2 in RTDS as a GOOSE subscriber. Any violation of the charging station voltage and frequency limits is detected by RTAC, which initiates the trip logic to restore the station voltage and frequency. The trip signals are received using the GTNET-GSE component with map signals in the corresponding .SCD file, as shown in Fig. 3.19.

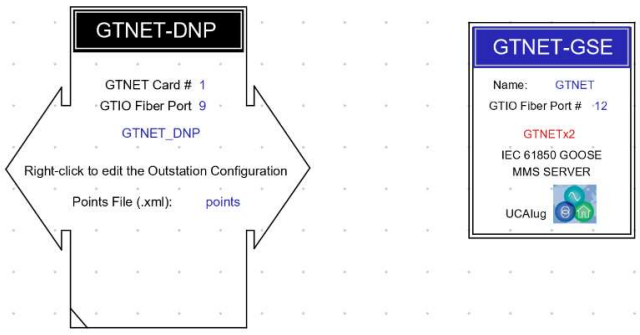

Fig. 3.19 GTNETx2 DNP and GOOSE component configuration in RSCAD draft.

The EV charging station status panel with the STNDBLK switch is shown in Fig. 3.20. A trip signal in the GOOSE message is issued to the charging station by the controller if any of the voltage or frequency limits are violated. The switch is used to manually de-block the EV charging station after the voltage and frequency have been restored. The LED indicators are used for Station ON (STN ON), Trip (STN Trip) and Overload (STNOL) status while the meters ST1P, ST1Q, ST2P, ST2Q ST3P, ST3Q, ST4P, ST4Q, ST5P and ST5Q reads the active and reactive power of the five charging stations, respectively (positive sign is for power OUT of the station into the grid, i.e., V2G mode of EVs). Upon the arrival of EVs, they charge/discharge in the station as per the schedule prepared by the PEV Scheduling Algorithm in TOU-based tariff in MATLAB received over SKT.

It is assumed that the total number of EVs, i.e., 580 (480 with Level 1 charging and 100 with Level 2 charging), are uniformly distributed to all the charging stations. As discussed earlier in this section, the EVs connected to charging stations 1 to 5 with different levels of initial SOC start charging/discharging as per the schedule prepared through the intelligent scheduling of the PEVs proposed in this work. Further, during the peak load hours, i.e., 1700hrs, EVs are connected to charging stations with different levels of SOC. A time-scaled voltage waveforms at the five charging stations at the time of connection of PEVs are inked in Fig. 3.21. The present work has considered maximum and minimum

voltage limits of 0.9 p.u. and 1.1 p.u., respectively (as mentioned in Table 3.3), which corresponds to Root Mean Square (RMS) voltage of 12.9kV and 15.8kV (peak voltage of 18.3kV and 22.4kV), respectively. It is observed from Fig. 3.21 that the peak voltage magnitude at all five charging stations is within these permissible voltage limits at 1700hrs if the proposed charging scheme is applied. Hence, the proposed charging scheme is able to avoid voltage variations as a result of EV connection at five charging stations. It can also be observed from Fig. 3.20 that as STNTrip LED is OFF for all the five charging stations, the RTAC controller issues no trip command during the entire charging period of EVs, and the GOOSE packets captured over Wireshark are shown in Fig. 3.22 wherein all the five EV charging station Trip Signal data is False. This further validates that the proposed charging scheme is able to keep voltage and frequency within permissible limits at all five charging stations.

It is observed from Fig. 3.20 that meter ST1P reads negative, whereas meters ST2P, ST3P, ST4P and ST5P read positive. It indicates that EVs at charging station 1 do not have sufficient initial SOC to discharge, whereas EVs at the other four charging stations can discharge at peak load hours (17:00h), thus helping in providing ancillary support to the grid. The power injected into the grid by five charging stations is shown in Fig. 3.23. It is observed from the figure that the power injected into the grid by charging station 1 is almost zero at 17:00h, whereas it is positive for the remaining four charging stations. EVs at charging station 1 neither charge (as it will deteriorate bus voltage) nor discharge (due to insufficient initial SOC) at this peak load hour. EVs at the other four charging stations discharge to provide ancillary services.

The cost of charging in the entire PEV schedule in the case of un-coordinated charging (i.e., charge at maximum rate as soon as EV is connected) is calculated to be $1050.39. In contrast, optimal charging of PEVs results in the overall charging cost to be $-13.78.

Negative charging cost indicates that the EV owners will earn instead of paying if the proposed charging scheme is adopted.

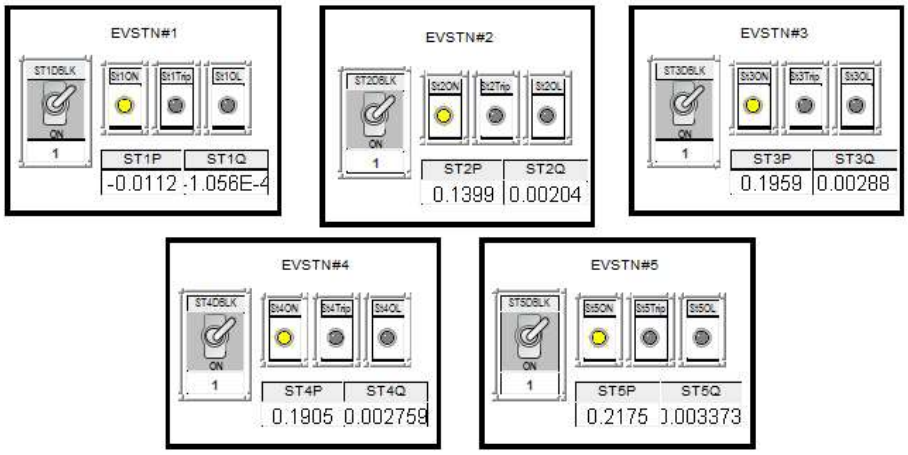

Fig. 3.20 EV Charging station status in RSCAD runtime at 1700hrs.

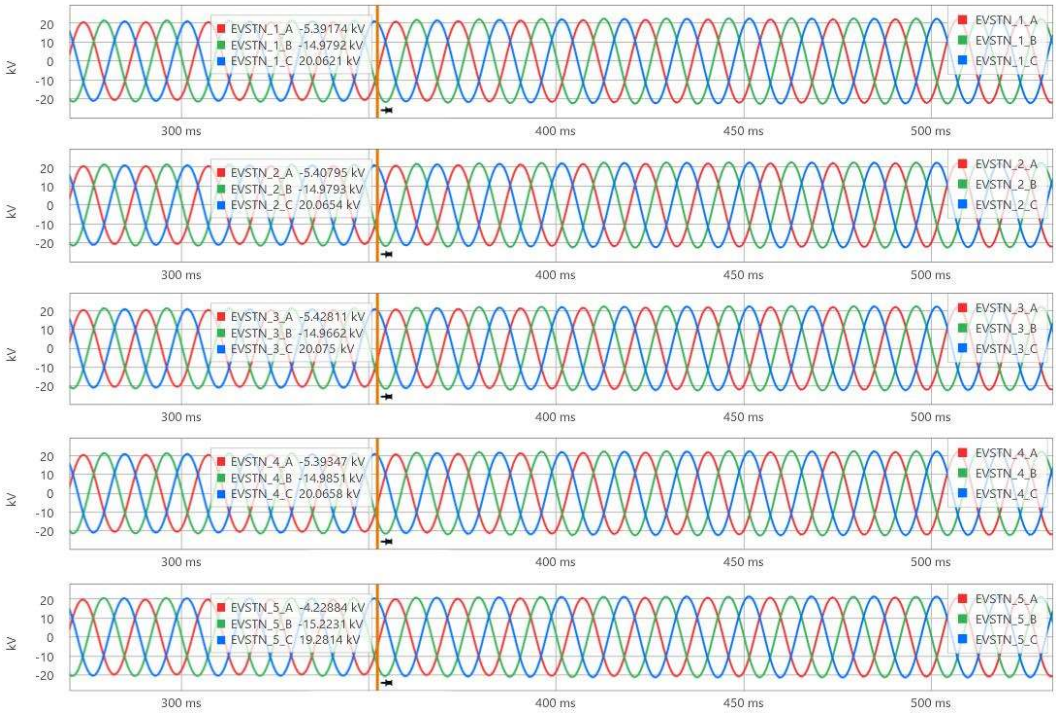

Fig. 3.21 EV charging station voltages from RSCAD runtime at the time of PEVs connection at 1700hrs (time-scaled).

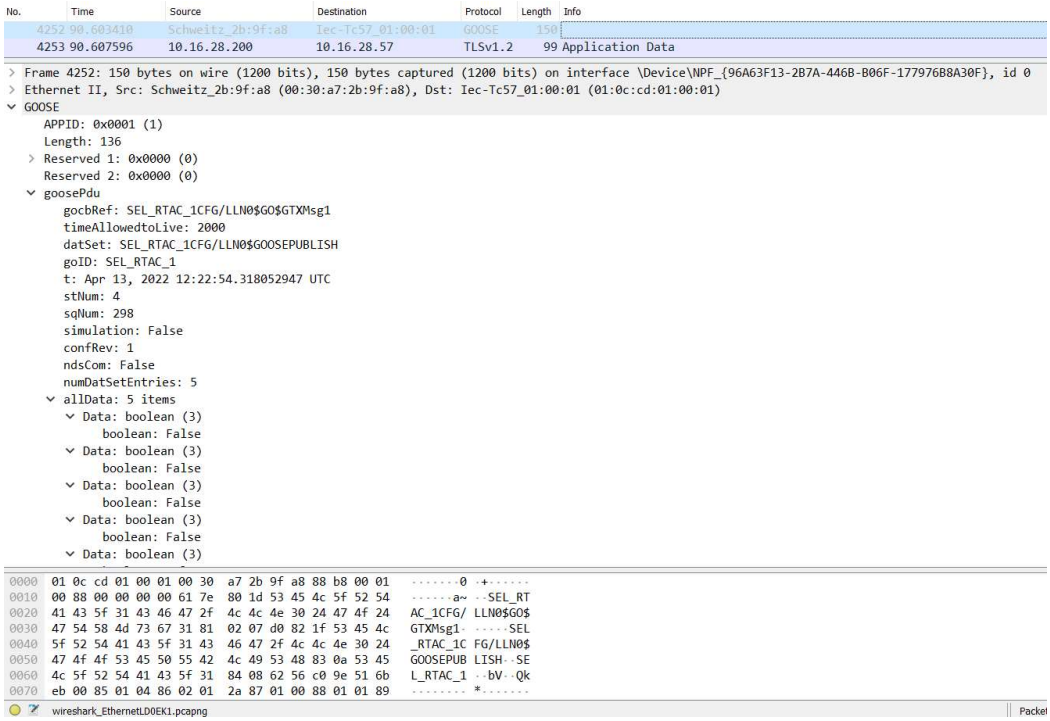

Fig. 3.22 GOOSE packets from RTAC received over Wireshark.

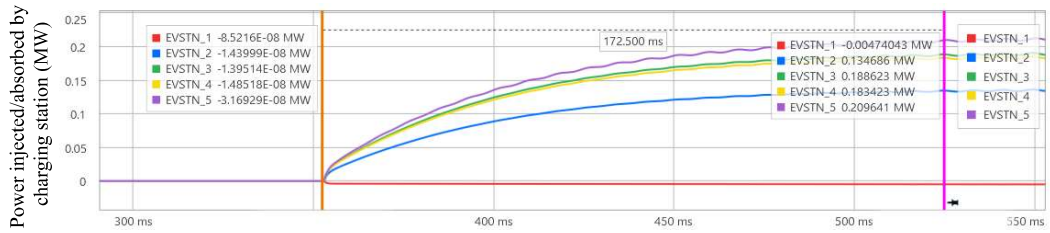

Fig. 3.23 EV charging station power from RSCAD runtime at the time of PEVs connection at 1700hrs (time-scaled).

3.6 RESULTS AND DISCUSSION

From the case study presented in Sections 3.4 and 3.5, the following observations and inferences are drawn:

1. It is observed from Fig. 3.5 (c) that the voltage profile resulting from the PEVs load could have deteriorated. However, shifting PEV charging from peak hours

to off-peak hours and their discharge during peak hours in a TOU-based tariff is able to restrain voltage deterioration.

2. As observed from Fig. 3.7, a slight variation in line parameters (increase in length of the line) forces the voltage at certain nodes to fall below the lower tolerance limits even without PEVs. The proposed PEV charging scheme schedules the PEVs to discharge in peak load hours and hence, brings back the voltage at all nodes into the tolerance limits (as shown in Fig. 3.8 (c)).

3. It is observed from Fig. 3.6 and Fig. 3.11 that an increase in the initial SOC of PEVs results in a reduction in charging cost for Test System I. The same is observed from Fig. 3.9 and Fig. 3.15 for Test System II. It is due to the reduction in charging time resulting from high initial SOC.

4. It is observed from Table 3.2 that the proposed PEV charging schedule under a TOU-based tariff provides a significant reduction in charging costs together with a reduction in voltage variability. Thus, the proposed EV charging scheme benefits EV owners as well as utilities by providing the ancillary service of voltage support in addition to the reduction in EV charging costs.

5. It is observed from Fig. 3.11 and Fig. 3.15 that EV charging under high initial SOC results in negative values of total charging cost. It indicates that EV owners earn a significant amount instead of paying if they are connected to charging stations with high values of initial SOC. This earning is higher for Test System I ($2.80) than Test System II ($2.76) as Test System II has voltage violations even in the absence of EVs connection that needs higher weightage to voltage variability reduction compared to Test System I.

6. The real-time feasibility of the proposed scheme is demonstrated in Section 3.6. RTAC issues trip command in case of violation of voltage and frequency limits at the charging station. As observed from Fig. 3.20 and Fig. 3.22, the charging station controller issues no trip command when EVs are charged with the proposed scheme. This indicates that all the voltages lie within the permissible limits, as observed in Fig. 3.21. Thus, real-time simulation results validate the proposed EV charging scheme's effectiveness in avoiding voltage variations due to the shifting of EV loads. As RTAC issues no trip command to the charging stations, all the constraints are satisfied during the entire period of EV charging.

7. It is observed from Fig. 3.23 that except for charging station 1, the remaining charging stations are able to provide ancillary services through power injection to the grid as EVs at those stations are at higher initial SOC.

Apart from the above-mentioned benefits, the proposed EV charging scheme has a few limitations, as presented below:

1. A higher penetration of EVs for a practical test system may lead to unfulfillment of the power balance constraints, and hence, an optimal schedule may not be achieved.

2. In the absence of TOU based tariff structure, the cost benefits of the EV owners will be reduced.

3. The higher cost benefits, as shown in Table 3.2, may be over-rated as the battery degradation cost is not considered in the problem formulation.

4. Further, the stochastic nature of arrival/departure times and driving patterns of the EVs is not considered in this work due to the deterministic nature of the formulated problem.

3.7 SUMMARY

A centralized approach was proposed in this chapter that minimizes the charging cost of PEVs and voltage deviations at buses for a study period of 24 hours. Under certain assumptions, a linear programming technique is employed for PEVs load scheduling over the available charging period. In the V2G scheme, PEVs with available energy in the battery assist the system voltage. The proposed scheme is evaluated on two test systems, and multiple cases are simulated. The obtained results confirm the efficiency of the proposed scheme wherein the PEVs with sufficient battery SOC were able to contribute to the system voltage and bring back the voltage at every node within the security limits. Further, another case was evaluated to highlight the benefits of the V2G scheme from the PEV owner's perspective. It was confirmed that in the TOU-based tariff structure, the PEV owner with sufficient initial SOC could profit by injecting power into the system during peak price hours. The scheme was successfully tested for real-time application in RTDS, and the results confirm the efficacy of the proposed approach.